

# NON-OSCILLATORY SPECTRAL ANALYSIS

## Elimination of Gibbs Phenomena from Reconstructed Piecewise Continuous Signals

Firmin Ndeges  
Electrical Engineering & Mathematics  
Virginia Tech

March 26, 2004

### Research Advisors

- Jeffrey T. Borggaard Associate Professor Interdisciplinary Center for Applied Mathematics Virginia Tech
- William T. Baumann Associate Professor Electrical and Computer Engineering Virginia Tech
- Terry L. Herdman Professor Interdisciplinary Center for Applied Mathematics Director Virginia Tech

Supporting Paper Used: Essentially Non-Oscillatory Spectral Fourier Methods for Shock Wave Calculations. By Wei Cai, David Gottlieb, and Chi-Wang Shu

### Abstract

Gibbs' phenomena occurs in Fourier approximation of piecewise continuous functions with discontinuities. This can lead to a number of practical difficulties including poor convergence behavior in approximations to nonlinear partial differential equations. A remedy for Gibbs phenomena was posed by Cai, Gottlieb and Shu (Essentially Non-Oscillatory Spectral Fourier Methods for Shock Wave Calculations). In their paper, they show that adding a discontinuous function to the standard trigonometric basis functions can mitigate the highly oscillatory phenomena that persists even as more terms are taken

In this work, we validate this method for the case of one discontinuity. We then extend the method for the case of multiple discontinuities. We begin by detailing an algorithm for selecting the appropriate basis functions to add to the (finite) trigonometric set using only Fourier coefficients of the discontinuous function. We then numerically validate our results for the case of two discontinuities, and derive a scheme for the case of three discontinuities or higher. Mathematical analysis is included that verifies our computed results.

We finally look at more practical issues, such as the sensitivity of our procedure to the magnitude and spacing of discontinuities. This study contains both numerical experimentation and supporting mathematical analysis.

## Historical Note about Gibbs Phenomenon

The traditional Fourier reconstruction of a discontinuous signal leads to fast oscillations near the location of the discontinuity point(s). This is known in the scientific world as the Gibbs phenomenon, in recognition to the one who first investigated and published this phenomenon. About 100 years ago, J. W. Gibbs proved that truncating the Fourier representation of a discontinuous signal introduces an overshoot error that cannot be reduced even if the number of terms that are used in the Fourier approximation is substantially increased.

## 1 Introduction

A discontinuous time signal whose spectral reconstruction from its Fourier coefficients displays no Gibbs phenomenon can be a valuable asset in the world of applied mathematics and engineering. This result can be used for example to get a better approximation of the conservation law Partial Differential Equation (PDE) listed below:

$$u_t + f(u)_x = 0. \tag{1}$$

Since this hyperbolic PDE may have a discontinuous solution, spectral approximation becomes much more complex because of the difficulty of working with the flux term  $f(u)_x$  close to a discontinuity.

The obstacle to finding accurate approximations to (1) is mainly due to the existence of the Gibbs phenomenon in our finite dimensional approximation  $u_N(x)$ . In a recently published paper by Cai, Gottlieb, and Shu [1], the authors develop a method to minimize the oscillations due to Gibbs and proceed with a more efficient way to find discontinuous solutions to PDEs. However, the paper only considered the case of one discontinuity, though it hinted that it could be extended to the case of multiple discontinuities.

The goal of this paper is to first verify the relevant results for the case of one discontinuity in our supporting paper. The intention here is not only to understand thoroughly what the method is all about, but also to illustrate why and how it works. Next, the application of the

non-oscillatory spectral analysis method is extended to the case of functions with multiple discontinuities. The paper concludes by listing a few domains of potential applications of the non-oscillatory spectral analysis method.

## 2 Structure of the Research

This report from the research work conducted on non-oscillatory spectral analysis is divided in two parts:

The first part consists of reviewing our supporting paper and becoming more familiar with all the concepts developed through that paper. The key results proved by our supporting paper are verified and additional explanations are provided whenever necessary. The central goal of this part is the elimination of Gibbs phenomenon for a function with one point of discontinuity by the use of the method illustrated in our supporting document.

Once familiar with all the concepts elaborated in the supporting paper, the next step is to try to extend the idea used in our supporting paper to eliminate Gibbs phenomenon for a function with multiple discontinuities. This is the novelty brought by the work presented here. The determination of the condition for a faster convergence in the case of a signal with two discontinuity points is examined, proved mathematically, and verified numerically.

The following equations, see for example [3], are used consistently throughout this research work:

$$P_N f(x) = \sum_{k=-N}^N \hat{f}_k e^{ikx}, \quad (2)$$

$$\hat{f}_k = \frac{1}{2\pi} \int_0^{2\pi} f(x) e^{-ikx} dx. \quad (3)$$

The terms *function* and *signal* are used interchangeably throughout the paper. FS stands for Fourier Series. A Few definitions about the notation for convergence used throughout the paper are shown below:

$$g(\epsilon) = O(\epsilon) \Rightarrow \lim_{\epsilon \rightarrow 0} \left[ \frac{g(\epsilon)}{\epsilon} \right] \text{ is finite,}$$

$$h(\epsilon) = O(\epsilon^2) \Rightarrow \lim_{\epsilon \rightarrow 0} \left[ \frac{h(\epsilon)}{\epsilon^2} \right] \text{ is finite.}$$

There may be a need to replace  $\epsilon$  by  $1/N$ , to obtain some of the results shown throughout this paper. One can easily see that:

$O(1)$  means that the phenomenon remains independent of  $N$ .

$O(1/N)$  means the phenomenon vanishes on the order of  $1/N$ . Gibbs is therefore an  $O(1)$  phenomena.

### 3 The Non-Oscillatory Spectral Reconstruction Method

The following notation is used throughout this part of our work

$u(x)$	: original function (signal) of interest with one point of discontinuity
$P_N u(x)$	: traditionally reconstructed signal that leads to Gibbs phenomenon
$u_{r_{\bar{u}N}}(x)$	: averaging cell $\bar{u}$ reconstructed from original $\hat{u}_l$
$u_{rN}$	: reconstructed signal from average cell formulation
$R_N u(x)$	: reconstructed combined signal with non-oscillatory behavior
$u_N(x)$	: final reconstructed signal with non-oscillatory spectral method
$x_s$	: true location of the discontinuity of $u$
$y$	: approximated location of the discontinuity of $u$
$[u]$	: true value of the jump at the point of discontinuity
$A$	: approximated value of the jump at the point of discontinuity

where the jump  $[u]$  is defined as

$$[u] = \frac{u(x_s^+) - u(x_s^-)}{2\pi}. \quad (4)$$

It is well known that the traditional spectral reconstruction of any discontinuous function leads to slow convergence near the discontinuity location of the reconstructed function. We have learned from Fourier analysis theory that the truncation of the infinite Fourier sum is what causes this oscillatory behavior. The method that is explored in the next few paragraphs successfully reconstructs a discontinuous signal with no oscillations near the point of discontinuity.

#### 3.1 Mathematical Approach

The slow convergence mentioned above is due to a specific term in the traditional Fourier reconstruction of the original signal. We choose to call that term  $f_l$  and it turns out to be a function of  $x_s$  and  $[u]$  as shown below. This choice of notation  $f_l$  will be understood later.

Assuming that the  $2N+1$  Fourier coefficients  $\hat{u}$  of  $u(x)$  are known, we will now attempt to derive an expression for our non-oscillatory spectral reconstruction of our original discontinuous signal  $u(x)$ .

One way of rewriting the expression of the Fourier coefficients  $\hat{u}_l$  as defined in (3) is:

$$\hat{u}_l = e^{-ilx_s} \sum_{k=0}^{n-1} \frac{[u^k]}{(il)^{k+1}} + \frac{1}{2\pi} \int_0^{2\pi} \frac{u^n}{(il)^n} e^{-ilx_s} dx. \quad (5)$$

Proof:

$$\begin{aligned}
\hat{u}_l &= \frac{1}{2\pi} \int_0^{2\pi} u(x)e^{-ilx} dx \\
&= \frac{1}{2\pi} \int_0^{x_s} u(x)e^{-ilx} dx + \frac{1}{2\pi} \int_{x_s}^{2\pi} u(x)e^{-ilx} dx \\
&= \frac{1}{2\pi} \left\{ \left[ \frac{u(x)e^{-ilx}}{-il} \right]_0^{x_s} - \frac{1}{-il} \int_0^{x_s} u'(x)e^{-ilx} dx \right\} \\
&\quad + \frac{1}{2\pi} \left\{ \left[ \frac{u(x)e^{-ilx}}{-il} \right]_{x_s}^{2\pi} - \frac{1}{-il} \int_{x_s}^{2\pi} u'(x)e^{-ilx} dx \right\} \\
&= \frac{1}{2\pi il} \left[ -u(x_s^-)e^{-ilx_s} + u(0^+) - u(2\pi)e^{-2\pi il} \right. \\
&\quad \left. + u(x_s^+)e^{-ilx_s} + \int_0^{2\pi} u'(x)e^{-ilx} dx \right],
\end{aligned}$$

since  $u$  is  $2\pi$  periodic, we must have  $u(2\pi) = u(0)$ . It then follows that:

$$\begin{aligned}
\hat{u}_l &= e^{-ilx_s} \frac{u(x_s^+) - u(x_s^-)}{2\pi il} + \frac{1}{2\pi} \int_0^{2\pi} \frac{u'(x)e^{-ilx}}{il} dx \\
&= e^{-ilx_s} \frac{u(x_s^+) - u(x_s^-)}{2\pi il} \\
&\quad + \frac{1}{2\pi} \int_0^{x_s} \frac{u'(x)e^{-ilx}}{il} dx + \frac{1}{2\pi} \int_{x_s}^{2\pi} \frac{u'(x)e^{-ilx}}{il} dx \\
&= e^{-ilx_s} \frac{u(x_s^+) - u(x_s^-)}{2\pi il} + e^{-ilx_s} \frac{u'(x_s^+) - u'(x_s^-)}{2\pi (il)^2} \\
&\quad + \int_0^{2\pi} \frac{u''(x)e^{-ilx}}{(il)^2} dx.
\end{aligned}$$

Using (4) here, we end up with:

$$\hat{u}_l = e^{-ilx_s} \sum_{k=0}^1 \frac{[u^k]}{(il)^{k+1}} + \frac{1}{2\pi} \int_0^{2\pi} \frac{u^{1+1}}{(il)^{1+1}} e^{-ilx} dx$$

The result, (5) then follows by induction.

At this point, note that all the terms in (5) are converging at a rate of at least  $1/l^2$ , except for the very first term when  $k = 0$ ; this is the slow converging term called  $f_l$  above. Therefore,

faster convergence for the reconstructed signal can be obtained as soon as there is a way to explicitly define  $f_l$  so that it can be extracted.

In order to find out more about the true nature of  $f_l$  when  $k = 0$ , let's consider the  $2\pi$  periodic sawtooth function defined over  $[0, 2\pi]$  by

$$F(x, x_s, A) = A \begin{cases} -x, & x \leq x_s, \\ 2\pi - x, & x > x_s. \end{cases} \quad (6)$$

From (3), it is easy to determine the Fourier coefficients of the sawtooth function. Then, (2) can be used to rewrite  $F(x, x_s, A)$  as shown below:

$$\begin{aligned} \hat{f}_k(x_s, A) &= A \frac{e^{-ikx_s}}{ik}, & |k| \geq 1, \\ \hat{f}_0(x_s, A) &= A(\pi - x_s). \end{aligned} \quad (7)$$

Since the jumps of the second and all the higher order derivatives of  $F$  with respect to  $x$  are all equal to zero ( $d^k F/dx^k = 0$  for  $k > 1$ ), one can predict that the sawtooth function  $F(x, x_s, A)$  has the same convergence pattern as the first term of the sum in (5). As a matter of fact, a simple numerical computation proves that the first term of that sum is exactly equal to the sawtooth function defined in (6) and reconstructed in (7).

The general Fourier Series expression of  $u$  then becomes:

$$\hat{u}_l = \hat{f}_l(x_s, [u]) + e^{-ilx_s} \sum_{k=1}^{n-1} \frac{[u^k]}{(il)^{k+1}} + \frac{1}{2\pi} \int_0^{2\pi} \frac{[u^n]}{(il)^n} e^{-ilx_s} dx. \quad (8)$$

Since  $f_l$  mentioned earlier leads to the contribution of the term  $\hat{f}_l(x_s, [u])$  in the expression above, the oscillations of first order that occur in the traditional reconstruction of discontinuous time signals are caused by the slow convergence of the contribution from the  $\hat{f}_l(x_s, [u])$  terms. These terms are the Fourier coefficients for the sawtooth function that have both their jump magnitude and location equal to the jump magnitude and the jump location of our original function  $u(x)$ . Therefore, we can minimize the oscillatory behavior of the reconstructed signal by trying to eliminate the components generated by  $\hat{f}_l(x_s, [u])$ .

One way to do this is to add another sawtooth function whose purpose is to cancel the contribution of  $\hat{f}_l(x_s, [u])$  for  $-N \leq l \leq N$  ( $l \neq 0$ ) in our overall reconstruction of  $u(x)$ . We choose to use the sawtooth function  $s(x)$  given by

$$\sum_{\substack{l=-\infty \\ l \neq 0}}^{\infty} \frac{A}{il} e^{-ily} e^{ilx} \quad (9)$$

and  $A(\pi - x_s)$  when  $l = 0$ . Here,  $y$  and  $A$  are respectively the approximated jump location ( $\sim x_s$ ) and magnitude of the discontinuity point ( $\sim [u]$ ). Combining the Fourier components of the two functions  $s(x)$  and  $u(x)$  during the reconstruction process into a new function given by:

$$R_N u(x) = a_0 + \sum_{\substack{|l| \leq N \\ l \neq 0}} a_l e^{ilx} + \sum_{|l| > N} \frac{A}{il} e^{-ily} e^{ilx}. \quad (10)$$

With the correct value of  $[u]$  and  $x_s$ , the new function in (10) is  $O(1/N^2)$  convergent and Gibbs phenomenon is non-existent.

Note: In an attempt to simplify notation, we have substituted the traditional Fourier coefficient  $\hat{u}_l$  of our traditionally truncated and reconstructed signal, as given in (3), by the term(s)  $a_l$  above. In other words:

$$P_N u(x) = \sum_{l=-N}^N a_l e^{ilx} \quad \text{and} \quad (11)$$

$$u(x) = \sum_{l=-\infty}^{\infty} \hat{u}_l e^{ilx}. \quad (12)$$

The next concern is about how to determine or approximate the jump location and its magnitude. A good path to follow is to explore the orthogonality properties of the basis functions of the Fourier series representation. Since the exponential form of the Fourier series is used throughout this work, the orthogonality of exponential functions is the main property exploited. Doing so, it follows:

$$\int_0^{2\pi} (u - R_N u) e^{-ikx} dx = 0, \quad |k| \leq N + 2. \quad (13)$$

$$\int_0^{2\pi} \left( \sum_{l=-\infty}^{\infty} \hat{u}_l e^{ilx} - \sum_{|l| \leq N} a_l e^{ilx} - \sum_{|l| > N} \frac{A}{il} e^{-ily} e^{ilx} \right) e^{-ikx} dx = 0, \quad |k| \leq N + 2. \quad (14)$$

For the terms  $l \neq k$ , we have:

$$\int_0^{2\pi} e^{ilx} e^{-ikx} dx = 0. \quad (15)$$

For the terms  $l = k \leq N$ ,

$$\hat{u}_l - a_l = 0. \quad (16)$$

This confirms the fact that  $R_N u(x)$  and  $u(x)$  have the same Fourier coefficients.

For the terms  $l = k > N$ , equation (14) becomes:

$$\hat{u}_l - \frac{A}{il} e^{-ily} dx = 0 \quad (17)$$

Using  $l = k = N + 1$  and  $l = k = N + 2$  respectively, we end up with:

$$\frac{A}{i(N+1)} e^{-i(N+1)y} = \hat{u}_{N+1}, \quad (18)$$

$$\frac{A}{i(N+2)} e^{-i(N+2)y} = \hat{u}_{N+2}. \quad (19)$$

The last step is to take the ratio of (18) and (19) to get an estimate of  $y$ ; the magnitude of  $A$  can be easily found from either equation using the fact that exponential functions have a magnitude of one. (18) or (19) determine the sign of  $A$  once its magnitude is known. Thus, the final results:

$$e^{iy} = \frac{(N+1)\hat{u}_{N+1}}{(N+2)\hat{u}_{N+2}}, \quad (20)$$

$$|A| = (N+1)|\hat{u}_{N+1}|. \quad (21)$$

The reconstruction of a function  $u(x)$  with one point of discontinuity is therefore possible by combining that function with a sawtooth function in their Fourier representations. The resulting function is essentially non-oscillatory as will be illustrated later by studying a numerical example. The successful removal of the term  $f_l$  with the slow convergence from our traditional Fourier representation of  $u$  has positively affected the total variation of our new function: while  $TV[P_N u]$  does not converge to  $TV[u]$ , especially near the point of discontinuity, an elaborate mathematical proof in [1] assures us that  $TV[u_N]$  converges to  $TV[u]$  with second order accuracy.

Our final reconstructed signal  $u_N$  is given by:

$$u_N(x) = a_0 + \sum_{\substack{l=-N \\ l \neq 0}}^N (\hat{u}_l - \frac{A}{il} e^{-ily}) e^{ilx} + F(x, y, A), \quad (22)$$

where  $F(x, y, A) = s(x)$  is the sawtooth function that is defined as in (6) and used in the non-oscillatory approximation effort.

A numerical verification of the above results seem to be the next logical step. However, we explore another theoretical approach beforehand.

## 3.2 Signals and Systems Theory Approach

In signal analysis, the theory states that the Fourier coefficient for the  $N^{th}$  harmonic of any given time signal  $u$  decreases in magnitude no faster than  $1/N$  if  $u$  has one or many points

of discontinuities [4]. The part that is even more interesting is that if the  $k^{\text{th}}$  derivative of  $u$  is the first derivative that contains a point of discontinuity, then the Fourier coefficients of  $u$  converge to zero at a rate proportional to  $1/N^{k+1}$ .

From the above observations, the following could be said: for a continuous function, the Fourier coefficients will approach zero as  $1/N^2$  if the first derivative has a point of discontinuity, or they will approach zero as  $1/N^3$  if the first derivative is continuous and the second derivative has a point of discontinuity.

This explains why the reconstruction of a continuous function is guaranteed to be at least  $1/N^2$  convergent and to be essentially non-oscillatory. A quantitative comparison between the Fourier coefficients of a triangular wave and the ones of a square wave makes the last point in convincing the reader in case there was still any doubt: the triangular wave is continuous and has its first derivative discontinuous; thus its Fourier coefficient can be predicted to be of the form  $C/N^2$ . On the other hand, the Fourier coefficient of the square wave out to be of the form  $D/N$  since the square wave is discontinuous in time.

Therefore, one can already see how and why the Gibbs phenomenon could be eliminated using the non-oscillatory spectral method analyzed throughout this paper. In fact, it is clear that transforming our discontinuous  $u(x)$  into a continuous function leads to a combined function with a faster convergence. The total variation of the combined signal  $u_N$  converges to the total variation of  $u$  to the second order and mitigates the highly oscillatory  $O(1)$  phenomena.

The discussion from the few paragraphs above indicates that the problem lies at the point of discontinuity  $x_s$ . Thus, our transformed function should be the combination of our original discontinuous function with a new function that can make  $u(x)$  continuous at that point  $x_s$ . Let  $s(x)$  be that function. In order to have a combined continuous function from a initial discontinuous one, we can certainly use a second function that is discontinuous at the same point  $x_s$  with the same jump of discontinuity in the same direction (the derivative of both function need to have the same sign). Once these conditions are met, a simple subtraction of the second function  $s(x)$  from our original signal  $u(x)$  gives us function  $u(x) - s(x)$  which is continuous at  $x_s$ .

One of simplest  $s(x)$  functions that meets these requirements is the sawtooth function, and since its Fourier coefficients are well-known and easy to work with, this method uses the sawtooth function to eliminate the oscillatory behavior in our combined reconstructed function.

Once the spectral analysis is complete, we can simply add the sawtooth  $s(x)$  that was subtracted from  $u(x)$ . This results in an essentially non-oscillatory reconstruction of the original signal  $u$ . The final reconstructed signal is therefore essentially non-oscillatory, even though it is a discontinuous signal.

### 3.3 Numerical Validation

#### 3.3.1 A discussion about the average cell formula

We define the cell average formula of  $u$  as:

$$\bar{u}(x, t) = \frac{1}{\Delta x} \int_{x-\frac{\Delta x}{2}}^{x+\frac{\Delta x}{2}} u(\xi, t) d\xi \quad (23)$$

Why do we care about it? While  $u(x)$  might not be continuous, the cell average formula defined in (1) is a continuous function. Therefore, if our main reason for using the non-oscillatory reconstruction method is to solve the PDE in (1), we can use our definition of  $\bar{u}$  to rewrite our PDE as:

$$\frac{\partial}{\partial t} \bar{u}(x, t) + \left[ \frac{1}{\Delta x} f(u(x + \frac{\Delta x}{2}, t)) - f(u(x - \frac{\Delta x}{2}, t)) \right] = 0 \quad (24)$$

and the initial condition  $u(x, 0) = u^0(x)$  of becomes:

$$\bar{u}(x, 0) = \bar{u}^0(x) \quad (25)$$

Assuming we are dealing with a conservative PDE, a numerical approach to solving the resulting equation above is:

$$\frac{d}{dt} \bar{u}_j = -\frac{1}{\Delta x} (\bar{f}_{j+1/2} - \bar{f}_{j-1/2}) \quad (26)$$

The form above allows to make use of the numerical flux  $\bar{f}_{j+1/2}$  in order to approximate  $f(u(x_j + \Delta x/2, t))$ . For this, we also need to have the values of  $u_{j+1/2}$ , but these can be estimated using the non-oscillatory reconstructed  $u_N$ ; i.e.,

$$\bar{f}_{j+1/2} = f(u_N(x_j + \Delta x/2, t)) \quad (27)$$

The left side of (26) can be approximated using the first order finite difference

$$\frac{d}{dt} \bar{u}(x, t) \approx \frac{\bar{u}(x, t + \Delta t) - \bar{u}(x, t)}{\Delta t}. \quad (28)$$

Note that for the remainder of this manuscript we are only interested in the spatial reconstruction of the solution and suppress the time variable  $t$ .

The last concern in this process is to know how to compute  $a_l$  from the  $\bar{a}_l$  Fourier coefficients of the cell average function  $\bar{u}$  as defined in (23).

Signals and Systems analysis comes back again. Observe a similarity between time marching of  $u$  to obtain  $\bar{u}$  and the concept of convolution; the numerical verification will validate this indeed. Basically,  $\bar{u}$  is obtained from  $u$  by convolving  $u$  with a narrow rectangular time pulse of width  $\Delta x$  and of height  $1/\Delta x$ .

After getting a good representation of  $\bar{u}(x)$ , its Fourier coefficients can be found by using (2). Let  $a_l$  and  $\bar{a}_l$  be respectively the Fourier coefficients of  $u(x)$  and  $\bar{u}(x)$ . Since convolution in the “time” ( $x$ ) domain leads to multiplication in the frequency domain, and because the equivalent of a rectangular pulse is a *sinc* function in the frequency domain, the Fourier coefficients  $a_l$  of  $u$  are then recovered from those of  $\bar{u}$  through the relation:

$$\bar{a}_l = \sigma_l a_l \tag{29}$$

The  $a_l$  values can be recovered from the above equation.  $\sigma_l$  is the equivalent of a rectangular pulse in the frequency domain; this is a *sinc* function and it can be defined as:

$$\sigma_l = \frac{\sin\left(\frac{l\Delta x}{2}\right)}{\left(\frac{l\Delta x}{2}\right)}. \tag{30}$$

In the example that follows,  $\bar{u}$  is used to reconstruct  $u_N$  for the sole purpose of showing that it works. In this specific case of the function chosen, there is no real need to go through  $\bar{u}$  to be able to successfully reconstruct the non-oscillatory function  $u_N(x)$  from the function  $u(x)$  used.

### 3.3.2 Numerical Example

For our first example, we consider Fourier approximation and the non-oscillatory reconstruction of the function:

$$u(x) = \begin{cases} \sin\left(\frac{x}{2}\right), & 0 \leq x \leq 0.9, \\ -\sin\left(\frac{x}{2}\right), & 0.9 < x < 2\pi. \end{cases} \tag{31}$$

These approximations will support the theoretical discussion of these approximations for a function with one discontinuity shown in figure 1. In figure 2, we demonstrate Gibbs phenomena using traditional Fourier approximation.

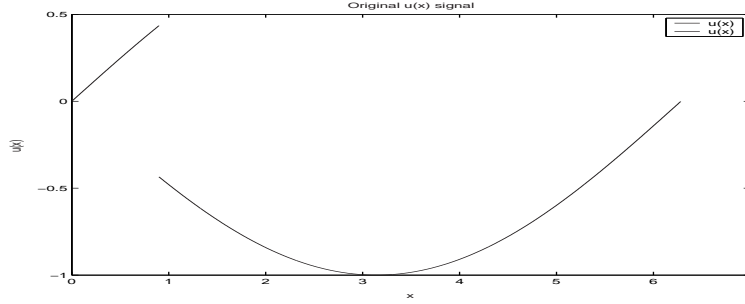


Figure 1: Plot of the function  $u(x)$

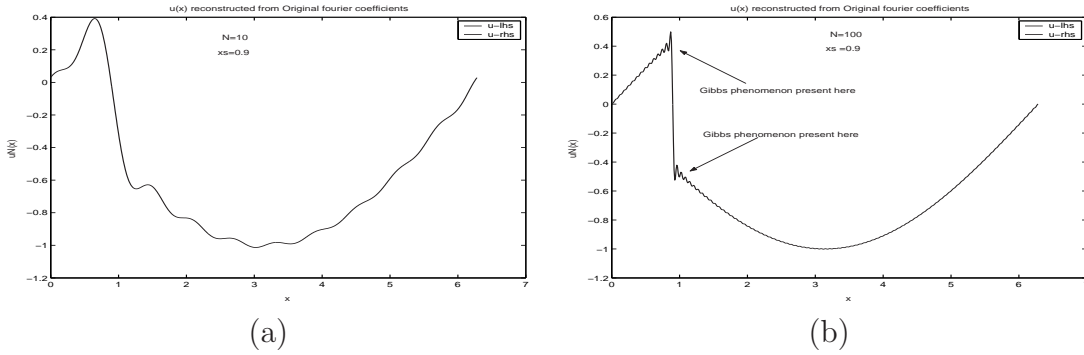


Figure 2: Traditionally reconstructed  $P_N u$ , (a)  $N = 10$  & (b)  $N = 100$

Figure 2 shows our signal traditionally reconstructed. While the case of  $N = 10$  might not show it well, it is obvious for  $N = 100$  that Gibbs phenomenon is present in that traditionally reconstructed signal.

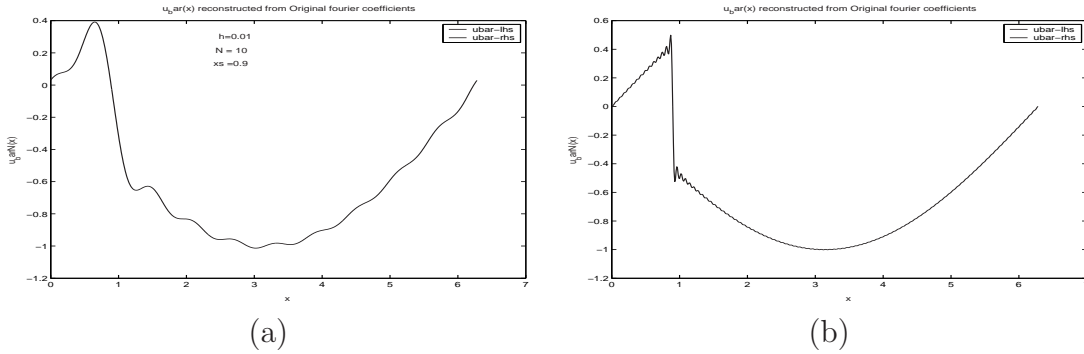


Figure 3: Plot of  $u_{r\bar{u}N}$  reconstructed from  $\hat{u}_l$ , (a)  $N = 10$  & (b)  $N = 100$

If we were to use this method for solving hyperbolic PDEs, we would need to reconstruct our signal  $u$  using  $\bar{u}(x)$  instead of using the Fourier coefficients  $\hat{u}_l$  of  $u$ . Fig 3 and fig 4 demonstrate that both reconstructions give identical results.

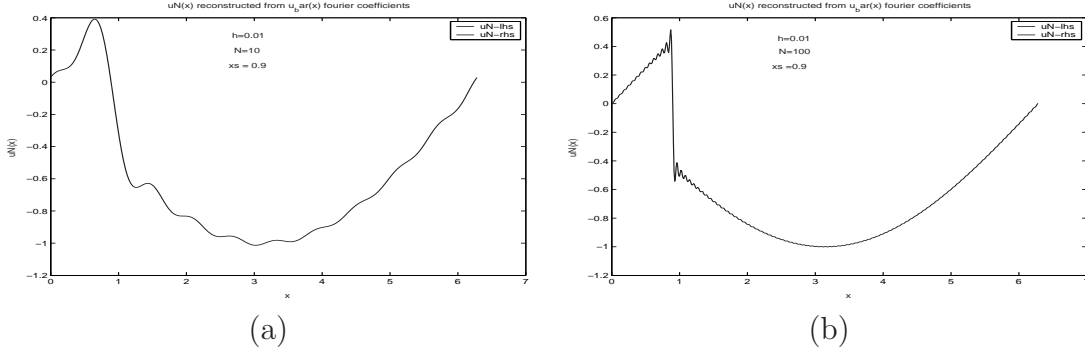


Figure 4: Plot of  $u_{rN}$  reconstructed from  $\bar{u}$ , (a)  $N = 10$  & (b)  $N = 100$

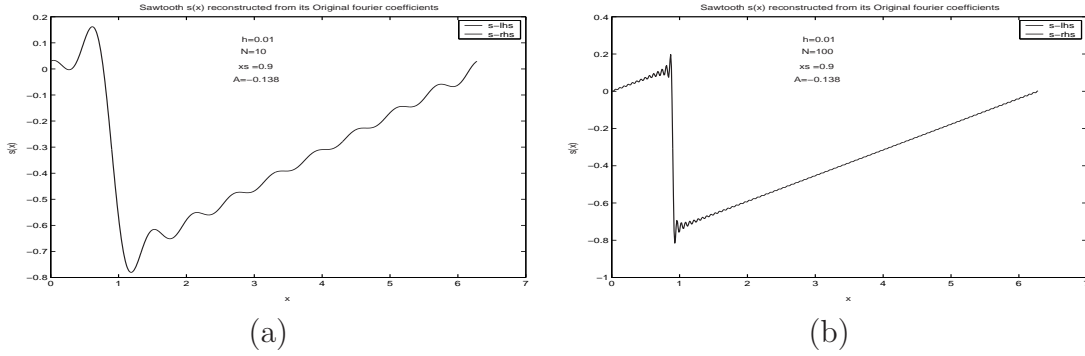


Figure 5: Plot of  $s(x)$ , (a)  $N = 10$  & (b)  $N = 100$

Figure 5 illustrates the sawtooth function used for the non-oscillatory reconstructions. The intermediate non-oscillatory reconstruction is displayed in figures 6.

The last step of our reconstruction process is to add back the sawtooth function we subtracted from  $u(x)$  to make the original function continuous. Here we are adding a continuous function to a discontinuous one. Since both function do not have any region of oscillation, the resulting final reconstruction  $u_N(x)$  will not present any point of oscillation, even near the point  $x_s$  of discontinuity.

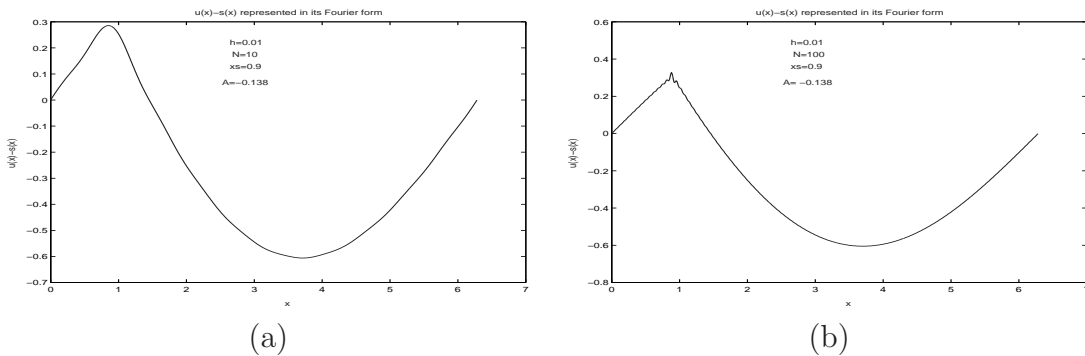


Figure 6: Plot of  $R_N u$ , (a)  $N = 10$  & (b)  $N = 100$

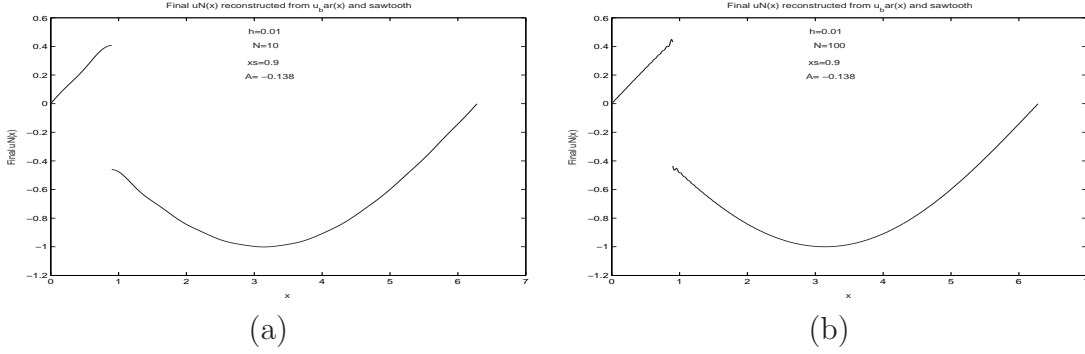


Figure 7: Plot of  $u_N(x)$ , (a)  $N = 10$  & (b)  $N = 100$

Figure 7 illustrates our final reconstructed  $u_N(x)$ . Therefore, with our new reconstruction method, we have successfully been able to eliminate the Gibbs phenomenon in this function  $u(x)$  that would naturally lead to the oscillations due to the Gibbs phenomenon when reconstructed in the traditional spectral fashion.

Remark: Even though the reconstruction matches the original function with very good accuracy, there is a mismatch in the shapes of both functions at the edge where the discontinuity occurs. Although this is mainly due to the fact that the  $y$  value used is an approximation of the exact value  $x_s$ , it can be shown that the mismatch is also caused by the difference between the derivative of our original function and the derivative of the sawtooth function that we used for our non-oscillatory reconstruction [2]

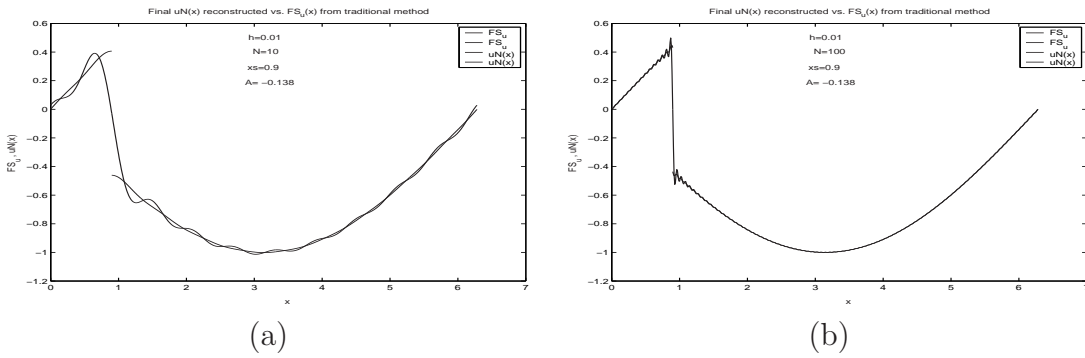


Figure 8: Plot of  $P_N u$  vs  $u_N$ , (a)  $N = 10$  & (b)  $N = 100$

Note that the mismatch just mentioned a few lines above causes the highest error as we can see in figures 8 and 9.

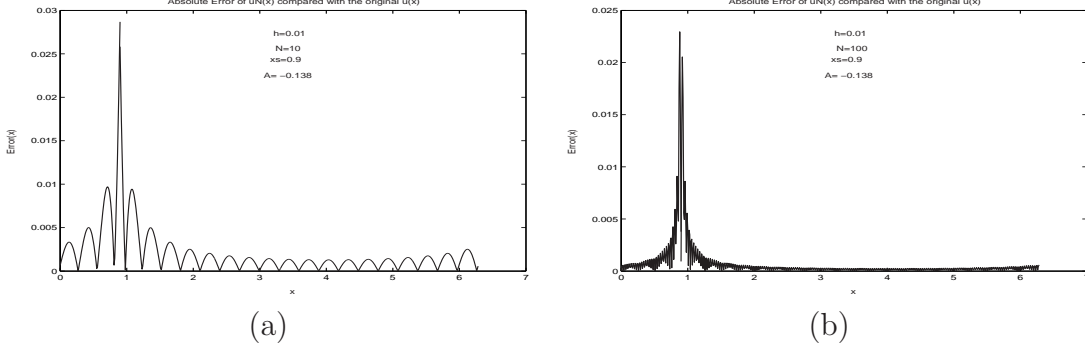


Figure 9: Plot of  $u_N(x) - u(x)$ , (a)  $N = 10$  & (b)  $N = 100$

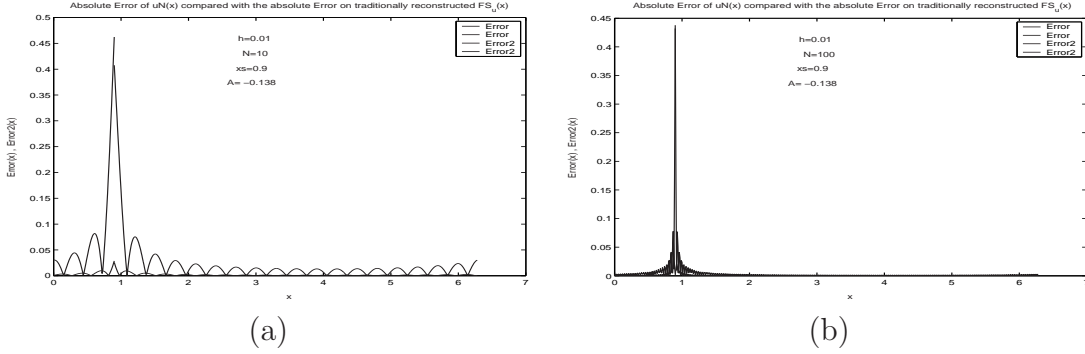


Figure 10: Plot of  $u_N(x) - P_N u(x)$ , (a)  $N = 10$  & (b)  $N = 100$

Figure 10 shows that as  $N$  grows larger, Absolute error grows smaller.

## 4 Expansion of the Method: Case of Multiple Discontinuities

The following notation is used throughout this part of our work

- $u(x)$  : original function (signal) of interest with one point of discontinuity
- $P_N u(x)$  : traditionally reconstructed signal that lead to Gibbs phenomenon
- $u_{r_{\bar{u}N}}(x)$  : averaging cell  $\bar{u}$  reconstructed from original  $\hat{u}_l$
- $u_{rN}$  : reconstructed signal from average cell formulation
- $R_N u(x)$  : reconstructed combined signal with non-oscillatory behavior
- $u_N(x)$  : final reconstructed signal with non-oscillatory spectral method
- $x_{s1}$  : true location of the first discontinuity of  $u$
- $x_{s2}$  : true location of the second discontinuity of  $u$
- $y_1$  : approximated location of the first discontinuity of  $u$
- $y_2$  : approximated location of the second discontinuity of  $u$
- $[u_1]$  : true value of the jump at the first point of discontinuity

- $[u_2]$  : true value of the jump at the second point of discontinuity
- $A_1$  : approximated value of the jump at the first point of discontinuity
- $A_2$  : approximated value of the jump at the second point of discontinuity

where the jumps  $[u_1]$  and  $[u_2]$  are defined as in (4)

From what we learned earlier, it is fair intuition to guess that eliminating the Gibbs phenomenon can be done in a similar reconstruction as in the case of one discontinuity by using two sawtooth functions that are discontinuous exactly at the same location as  $u(x)$  and that have the same jump values as  $u$  at those points of discontinuity. This should lead to an essentially non-oscillatory reconstructed solution  $u(x)$ .

However, for all this to be possible and before we proceed with numerical verification of our speculations, we need to examine the possibility of an extension of the mathematical proofs that we used for one discontinuity to work for the case of two discontinuities as well.

## 4.1 Mathematical Proofs and Theoretical Results

Based on the presentation in the first part of this work, the proof here is as concise as possible since all the extra-steps can be found in the first case. Only the key element that need to be verified in order to extend the method are taken into account.

First, since now we are dealing with a function that has two points of discontinuity, intuition based on the results from the case of one discontinuity tells us that we will need to use two sawtooth functions during our spectral analysis, in the similar fashion we did in the case of one discontinuity, for our final reconstruction of  $u$  to be essentially non-oscillatory. One of the key question however is: *“how can the locations as well as the magnitudes of the discontinuity be evaluated” for the case of a function with two discontinuity points?*

Based on the mathematical approach from the case with one discontinuity, it is easy to see that there are two terms that cause the slow convergence for a function with two points of discontinuity. This is seen by rewriting the fourier coefficients of our function  $u(x)$  in a similar form as in (5) and by defining two sawtooth functions as in (6) and (7). It then follows that:

$$\begin{aligned}
 \hat{u}_l &= \hat{f}_{l1}(x_{s_1}, [u_1]) + \hat{f}_{l2}(x_{s_2}, [u_2]) \\
 &+ e^{-ilx_{s_1}} \sum_{k=1}^{n-1} \frac{[u_1^k]}{(il)^{k+1}} + \frac{1}{2\pi} \int_0^{2\pi} \frac{u_1^n}{(il)^n} e^{-ilx_{s_1}} dx \\
 &+ e^{-ilx_{s_2}} \sum_{k=1}^{n-1} \frac{[u_2^k]}{(il)^{k+1}} + \frac{1}{2\pi} \int_0^{2\pi} \frac{u_2^n}{(il)^n} e^{-ilx_{s_2}} dx.
 \end{aligned} \tag{32}$$

The oscillation in the traditionally reconstructed  $P_N u(x)$  is caused by the slow convergence of the two terms:

$$F_{1N}(x, x_{s_1}, [u_1]) = \sum_{l=-N}^N \hat{f}_1(x_{s_1}, [u_1]) e^{ilx}. \quad (33)$$

$$F_{2N}(x, x_{s_2}, [u_2]) = \sum_{l=-N}^N \hat{f}_2(x_{s_2}, [u_2]) e^{ilx}. \quad (34)$$

Therefore, we will need an expansion of the form:

$$R_N u(x) = a_0 + \sum_{\substack{|l| \leq N \\ l \neq 0}} a_l e^{ilx} + \sum_{|l| > N} \frac{A_1}{il} e^{-ily_1} e^{ilx} + \sum_{|l| > N} \frac{A_2}{il} e^{-ily_2} e^{ilx} \quad (35)$$

Using the orthogonality condition and the orthogonal properties of the exponential function, we have next:

$$\int_0^{2\pi} (u - R_N u) e^{-ikx} dx = 0, \quad |k| \leq N + 4. \quad (36)$$

Just as in the case of one discontinuity, we re-define  $P_N u(x)$  as a function of  $a_l$  terms. This leads to:

$$\begin{aligned} \int_0^{2\pi} & \left( \sum_{l=-\infty}^{\infty} \hat{u}_l e^{ilx} - \sum_{|l| \leq N} a_l e^{ilx} - \sum_{|l| > N} \frac{A_1}{il} e^{-ily_1} e^{ilx} \right. \\ & \left. - \sum_{|l| > N} \frac{A_2}{il} e^{-ily_2} e^{ilx} \right) e^{-ikx} dx = 0, \quad |k| \leq N + 4. \end{aligned} \quad (37)$$

Just as in the case of one discontinuity again, we could have predicted the following three cases:

For the terms  $l \neq k$ , we have:

$$\int_0^{2\pi} e^{ilx} e^{-ikx} dx = 0 \quad (38)$$

For the terms  $l = k \leq N$ ,

$$\hat{u}_l - a_l = 0 \quad (39)$$

This confirms the fact that  $R_N u(x)$  and  $u(x)$  have the same Fourier coefficients.

For the terms  $l = k > N$ , equation (14) becomes:

$$\hat{u}_l - \frac{A_1}{il} e^{-ily_1} - \frac{A_2}{il} e^{-ily_2} = 0 \quad (40)$$

Therefore, using  $l = N + 1$ ,  $l = N + 2$ ,  $l = N + 3$  and  $l = N + 4$  respectively, we end up with the following system of four nonlinear equations with four unknowns:

$$\left\{ \begin{array}{l} \hat{u}_{N+1} = \frac{A_1}{(N+1)i} e^{-i(N+1)y_1} + \frac{A_2}{(N+1)i} e^{-i(N+1)y_2} \\ \hat{u}_{N+2} = \frac{A_1}{(N+2)i} e^{-i(N+2)y_1} + \frac{A_2}{(N+2)i} e^{-i(N+2)y_2} \\ \hat{u}_{N+3} = \frac{A_1}{(N+3)i} e^{-i(N+3)y_1} + \frac{A_2}{(N+3)i} e^{-i(N+3)y_2} \\ \hat{u}_{N+4} = \frac{A_1}{(N+4)i} e^{-i(N+4)y_1} + \frac{A_2}{(N+4)i} e^{-i(N+4)y_2} \end{array} \right. \quad (41)$$

Since the resulting system is nonlinear, an optimization toolbox can be used in Matlab for finding the solutions  $A_1$ ,  $A_2$ ,  $y_1$  and  $y_2$  of the system; we could for example use the Newton algorithm applied to systems of nonlinear equations for this. Another approach is to use Mathematica and let its Root Finder capability help us approximate the solutions of the system  $A_1$ ,  $A_2$ ,  $y_1$  and  $y_2$ . The results from numerical examples in this paper are based on results from Mathematica, since is a better and easier software than Matlab for symbolic operations.

Once obtained, the system of 4 non-linear equations with 4 unknowns is used to estimate the values of  $A_1$ ,  $A_2$ ,  $y_1$ , and  $y_2$ . These estimated values are used to determine the two sawtooth functions and proceed with the non-oscillatory reconstruction. From this point on, the procedure is exactly the same as in the case of a function with only one discontinuity. The resulting reconstructed function is essentially non-oscillatory and presents a faster convergence even near  $y_1$  and  $y_2$  as the Gibbs phenomenon is now non-existent.

Our final reconstructed signal  $u_N$  is given by:

$$\begin{aligned} u_N(x) = & a_0 + \sum_{\substack{l=-N \\ l \neq 0}}^N \left( \hat{u}_l - \frac{A_1}{il} e^{-ily_1} - \frac{A_2}{il} e^{-ily_2} \right) e^{ilx} \\ & + F_1(x, y_1, A_1) + F_2(x, y_2, A_2), \end{aligned} \quad (42)$$

where  $F(x, y_1, A_1) = s_1(x)$  and  $F_2(x, y_2, A_2) = s_2(x)$  are the two sawtooth functions whose locations and magnitudes of discontinuity match the ones of the original signal. These two sawtooth functions are defined as in (6), and they are used during the non-oscillatory approximation process.

One way to verify that the reconstructed signal is essentially non-oscillatory is to compare the total variation of the reconstructed signal  $u_N(x)$  with the total variation of the original signal  $u(x)$ .

The total variation of a function  $u$  over an interval  $[0, 2\pi]$  is defined as:

$$TV[u] = \sup_{P_i} \sum_{i=1}^n |u(x_i) - u(x_{i-1})|, \quad (43)$$

where  $P_i$  is the set of all partitions on  $x$ .

While it can be easily shown that the total variation of a sawtooth function  $F$  is  $4\pi$ , any book in Fourier analysis proves that  $TV[F_N] = O(\log(N))$ , where  $F_N$  is the Fourier reconstruction of the sawtooth. This discrepancy will turn out helpful for the TV of our reconstructed signal  $u_N(x)$ .

The proof below follows the model illustrated in [1] for the case of one discontinuity. In an attempt to avoid writing an excessive amount of algebraic manipulation, we will only display the important steps towards the final result.

We start by first remarking that we can rewrite (43) as:

$$TV[u] = \int_0^{2\pi} u'(\xi) d\xi. \quad (44)$$

Based on (32), the original function  $u$  can be rewritten as:

$$\begin{aligned} u(x) &= \hat{f}_{l1}(x_{s_1}, [u_1]) + \hat{f}_{l2}(x_{s_2}, [u_2]) \\ &\quad + \hat{S}_{l1}(x_{s_1}, [u'_1]) + \hat{S}_{l2}(x_{s_2}, [u'_2]) + g_1(x) + g_2(x), \end{aligned} \quad (45)$$

where  $g_1(x)$  and  $g_2(x)$  are defined as:

$$g_1(x) = e^{-ilx_{s_1}} \sum_{k=2}^{n-1} \frac{[u_1^k]}{(il)^{k+1}} + \frac{1}{2\pi} \int_0^{2\pi} \frac{u_1^n}{(il)^n} e^{-ilx_{s_1}} dx, \quad (46)$$

$$g_2(x) = e^{-ilx_{s_2}} \sum_{k=2}^{n-1} \frac{[u_2^k]}{(il)^{k+1}} + \frac{1}{2\pi} \int_0^{2\pi} \frac{u_2^n}{(il)^n} e^{-ilx_{s_2}} dx. \quad (47)$$

It follows that:

$$\begin{aligned} P_N u(x) &= F_{N1}(x, x_{s_1}, [u_1]) + F_{N2}(x, x_{s_2}, [u_2]) + S_{N1}(x, x_{s_1}, [u'_1]) \\ &\quad + S_{N2}(x, x_{s_2}, [u'_2]) + P_{N1}g_1(x) + P_{N2}g_2(x). \end{aligned} \quad (48)$$

The above represents our traditional reconstructed signal. In order to get the non-oscillatory spectral reconstruction behavior, we need a reconstructed signal  $u_N(x)$  defined as in the case of one discontinuity by:

$$\begin{aligned} u_N(x) = & P_N u(x) + F_1(x, y_1, A_1) - F_{N1}(x, y_1, A_1) \\ & + F_2(x, y_2, A_2) - F_{N2}(x, y_2, A_2), \end{aligned} \quad (49)$$

or

$$\begin{aligned} u_N(x) = & F_{N1}(x, x_{s1}, [u_1]) + F_{N2}(x, x_{s2}, [u_2]) + S_{N1}(x, x_{s1}, [u'_1]) \\ & + S_{N2}(x, x_{s2}, [u'_2]) + P_N g_1(x) + P_N g_2(x) + F_1(x, y_1, A_1) \\ & + F_2(x, y_2, A_2) - F_{N1}(x, y_1, A_1) - F_{N2}(x, y_2, A_2). \end{aligned} \quad (50)$$

Using simple algebraic manipulation, we end up with:

$$\begin{aligned} u_N(x) = & F_{N1}(x, x_{s1}, [u_1]) - F_{N1}(x, y_1, A_1) \\ & + F_{N2}(x, x_{s2}, [u_2]) - F_{N2}(x, y_2, A_2) \\ & + F_1(x, y_1, [u_1]) + S_1(x, y_1, [u'_1]) + g_1((x - y_1 + x_{s1})) \\ & + F_2(x, y_2, [u_2]) + S_2(x, y_2, [u'_2]) + g_2((x - y_2 + x_{s2})) \\ & + S_{N1}(x, x_{s1}, [u'_1]) - S_{N1}(x, y_1, [u'_1]) + P_N g_1(x) - g_1(x - y_1 + x_{s1}) \\ & + S_{N2}(x, x_{s2}, [u'_2]) - S_{N2}(x, y_2, [u'_2]) + P_N g_2(x) - g_2(x - y_2 + x_{s2}) \\ & + F_1(x, y_1, A_1) - F_1(x, y_1, [u_1]) \\ & + F_2(x, y_2, A_2) - F_2(x, y_2, [u_2]). \end{aligned} \quad (51)$$

Since we know:

$$u(x - y_1 + x_{s1}) = F_1(x, y_1, [u_1]) + S_1(x, y_1, [u'_1]) + g_1(x - y_1 + x_{s1}), \quad (52)$$

and

$$u(x - y_2 + x_{s2}) = F_2(x, y_1, [u_2]) + S_2(x, y_2, [u'_2]) + g_2(x - y_2 + x_{s2}), \quad (53)$$

combining (45), (46) and (46) with the extension of Lemma 3, 4, and 5 from our supporting paper [1], obtain:

$$\begin{aligned} TV[u_N] \leq & TV[u] + L_0 \frac{\log N}{N} + L_{11} \Delta_{11} N \log N + L_{21} \Delta_{21} \log N \\ & L_{12} \Delta_{12} N \log N + L_{22} \Delta_{22} \log N, \end{aligned} \quad (54)$$

where

$$\begin{aligned}\Delta_{1_1} &= |y_1 - x_{s1}|, & \Delta_{1_2} &= |y_2 - x_{s2}|, \\ \Delta_{2_1} &= |A_1 - [u_1]|, & \Delta_{2_2} &= |A_2 - [u_2]|.\end{aligned}$$

Since we know from a straight forward extension of theorem 2 in [1] that the four  $\Delta$  terms defined above are  $O(1/N^2)$ , (54) becomes:

$$TV[u_N] \leq TV[u] + K \frac{\log N}{N}, \quad (55)$$

where  $K$  depends on  $L_0, L_{1_1}, L_{1_2}, \Delta_{1_1}, \Delta_{1_2}$

Therefore, the total variation of our reconstructed signal  $u_N$  converges to the total variation of our original function  $u$ , in the case of a piecewise continuous signal with two discontinuities located at  $x_{s1}$  and  $x_{s2}$ .

This concludes the proof of the validity of the non-oscillatory spectral reconstruction method extended to the case of two discontinuities.

## 4.2 Numerical Validation

Below is the example we used for the second part of this research in order to validate the extension of the non-oscillatory spectral reconstruction method to the case of a signal with two points of discontinuities.

Example used:

$$u(x) = \begin{cases} \sin(\frac{x}{2}), & 0 \leq x \leq 0.9, \\ -\sin(\frac{x}{2}), & 0.9 < x < 2\pi - 0.9, \\ \sin(\frac{x}{2}), & 2\pi - 0.9 \leq x \leq 2\pi. \end{cases} \quad (56)$$

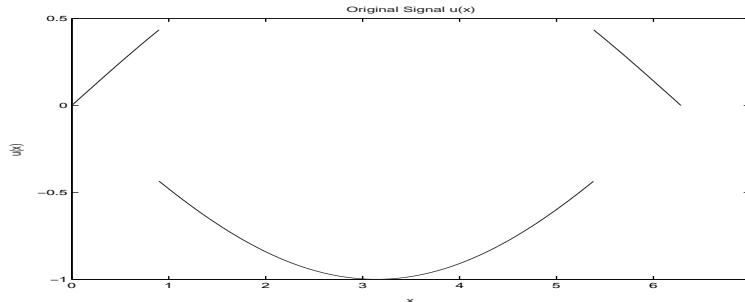


Figure 11: Plot of the original function  $u(x)$

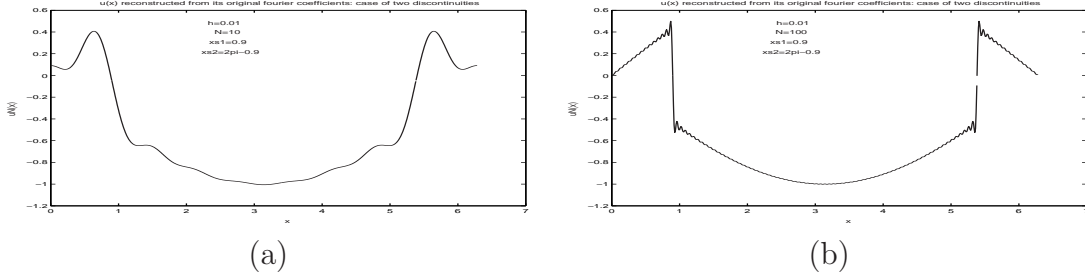


Figure 12: Plot of  $Pu_N(x)$ , (a)  $N = 10$  & (b)  $N = 100$

Even though the case  $N = 10$  in figure 12 might not clearly portray it, the case  $N = 100$  clearly illustrates that Gibbs phenomena is present in the traditionally reconstructed signal.

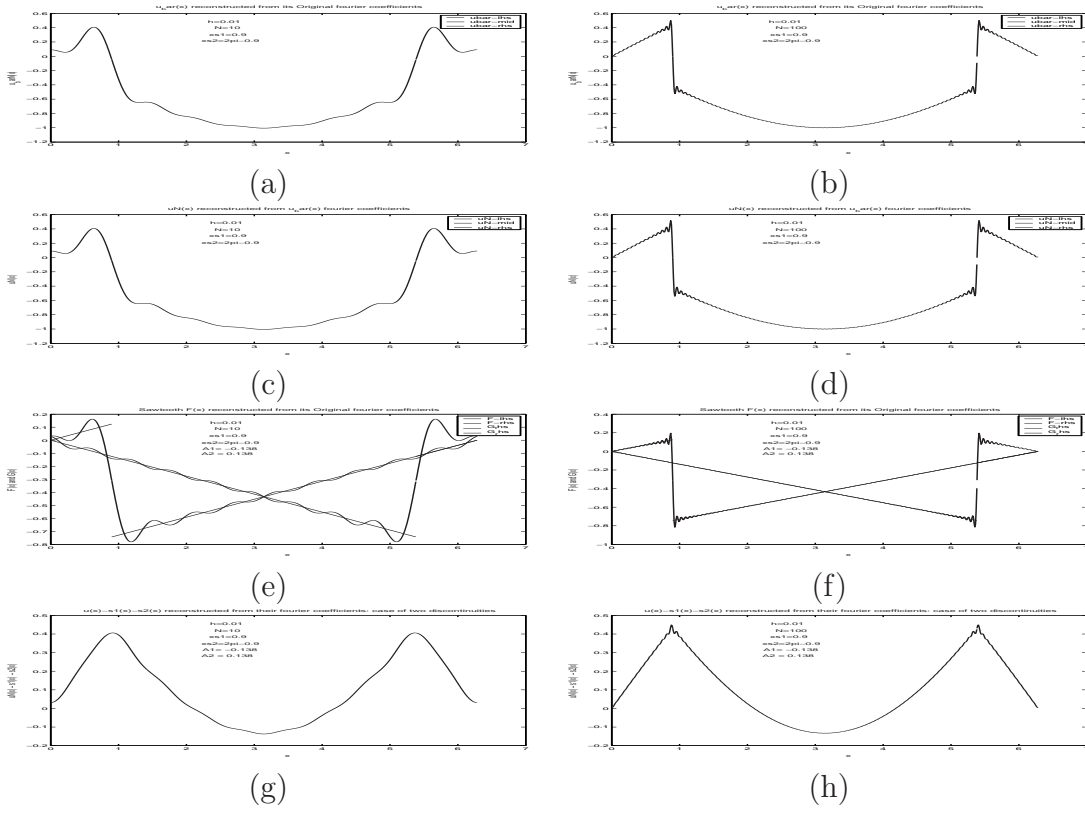


Figure 13: Rows 1 through 4 show the plots of  $\bar{u}(x)$ ,  $u_r(x)$ ,  $s(x)$  &  $Ru_N(x)$  respectively. (a), (c), (e) and (g) represent  $N = 10$  & (b), (d), (f) and (h) are for  $N = 100$

The method the paper is presenting to reconstructs  $u_N(x)$  in such a fashion that the oscillations resulting from the Gibbs phenomenon are totally eliminated as is shown in figures 13(a)-(h).

The newly reconstructed  $u_N(x)$  converges faster and has no observable Gibbs phenomenon, see figure 14.

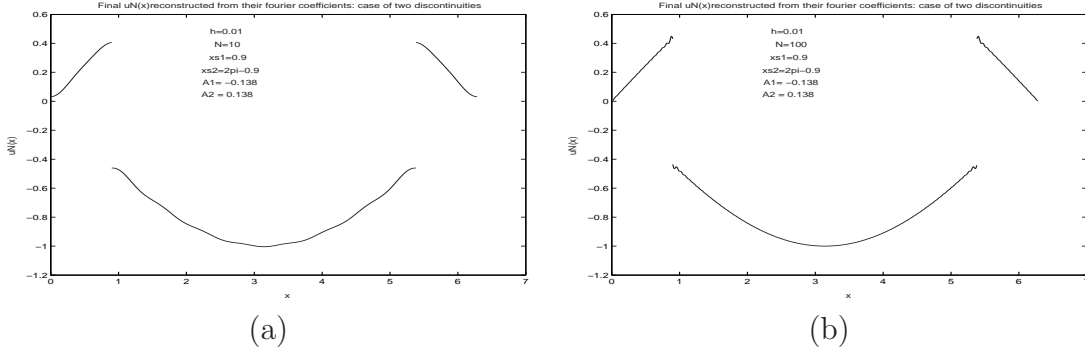


Figure 14: Plot of  $u_N(x)$ , (a)  $N = 10$  & (b)  $N = 100$

Figure 15(a)-(b) shows the reconstructed signal obtained using both our method and the traditional spectral methods. The error is displayed in figure 15(c)-(d).

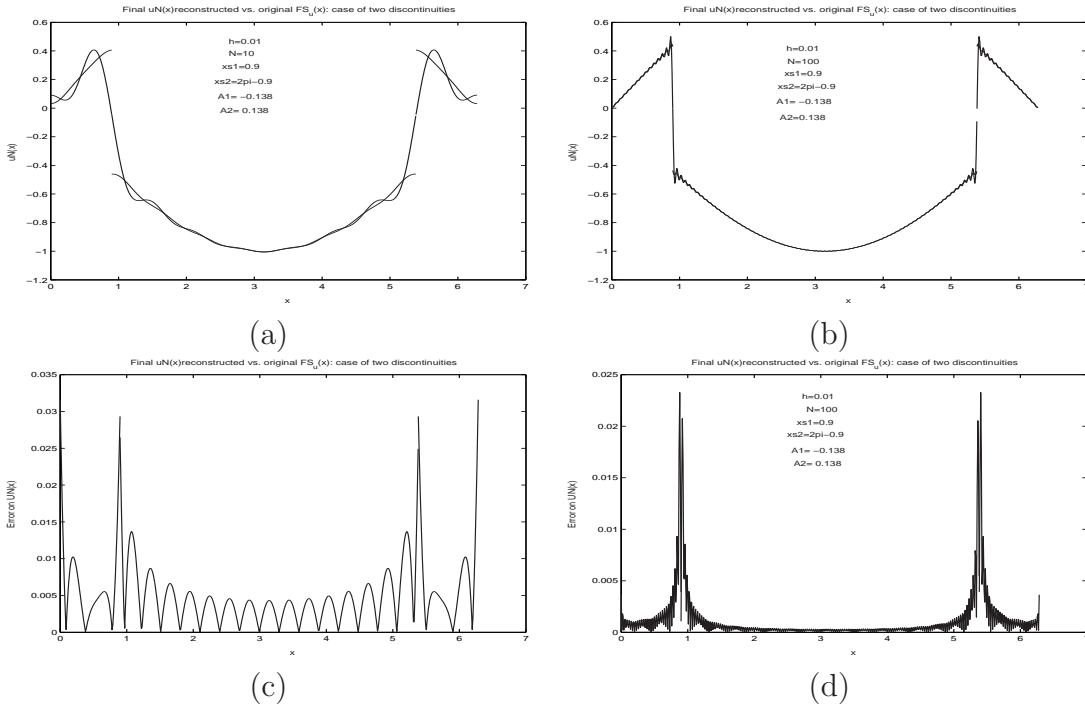


Figure 15: Row 1, plot of  $Pu_N(x)$  and  $u_N(x)$ . Row 2 shows the Error, (a) and (c) represent  $N = 10$ , (b) and (d) are for  $N = 100$

The results obtained and observations made on  $\bar{u}(x)$  for the one-discontinuity case also apply for the case of two-discontinuities.

### 4.3 Moving the discontinuity points closer

It was noticed that, as a general rule, the reconstructed signal would converge faster as the points of discontinuity moved closer up to a certain point. Then the pattern was quickly

lost, and an explanation for this is that with the discontinuity points too close to each other, other factors started coming into play and the error started getting bigger if we got any closer. We were not able to notice a pattern between the for optimal distance for the finest convergence, since it was all dependent on both the locations and the magnitudes of the gain as well as on the function used. Through numerous studies, we could not find an obvious pattern.

Therefore, as the discontinuity points move closer, whether or not the reconstruction  $u_N(x)$  is found to converge to  $u(x)$  faster is an area that will require further exploration in the future.

One problem faced in this section is the fact that the predicted behavior of the overall reconstructed solution when the two discontinuity points are moved closer really depends on the the specific function we are using.

#### 4.4 As number of discontinuity points grows larger

The steps for reconstructing an essentially non-oscillatory function from a p-piecewise function are the same as in the case of two discontinuities.

- Combine the original signal fourier coefficients with those of p sawtooth functions whose discontinuity magnitudes and locations match the discontinuity locations and magnitudes of our original function.
- Extend the orthogonality condition: finding the magnitudes and locations of the discontinuities Solving a system of  $2p$  nonlinear equations with  $2p$  unknowns
- Reconstructed  $u_N(x)$  Adding back the p sawtooth functions at the end of the reconstruction.

Considering the unstable behavior in the rate of convergence of the reconstructed signal that occurs when two points of discontinuity are moved too close to each other, it is fair to state that the method will be limited to a certain maximum number of p discontinuity points to produce acceptable results. In other words, research in nonlinear solvers for this problem is necessary for the reconstruction technique to be practical for large numbers of discontinuities.

## 5 Conclusion

The non-oscillatory spectral analysis method is a good way to transform a piecewise continuous function into a reconstructed equivalent that does not display the well-known Gibbs phenomenon around the location of each discontinuity. The main steps of the methods are:

1. Compute the Fourier coefficients of the given function. Use the average cell formulation of the original function if needed to find the Fourier representation of the original function.
2. Determine the location and magnitude of the jumps using the orthogonality properties of the basis functions used in the Fourier representation. Then use a non-linear equation solver to find an accurate estimate of the locations and the magnitudes of the jumps in the original function.
3. Use as many sawtooth functions as there are discontinuities on the original function. The jump locations and magnitudes for each sawtooth chosen to match the estimated jump locations and magnitudes of our original function.
4. Compute  $u_N(x)$  by combining the original function and the sawtooth functions in their respective Fourier representations.
5. Add back the sawtooth functions to the combined reconstructed function  $R_N(x)$  to get the final reconstructed solution  $u_N(x)$  of our original function.

Below is a short discussion about some areas where this non-oscillatory spectral analysis method finds valuable applications.

In Mathematics, the non-oscillatory spectral reconstruction method can be used to solve conservation laws of the form  $u_t + f(u)_x = 0$ . Things get simpler with the help of this method in attaining a sustainable solution of the PDE, and the average cell formula is used whenever necessary. Refer to [2] for further details.

In Aerospace Engineering, this method is used for shock wave calculations. Refer to [1] for further details.

Since this spectral analysis method eliminates Gibbs phenomenon from reconstructed discontinuous signals, another possible domain of applications is found in the Window Function technique design of Finite Impulse Response (FIR) filter. In fact, one concern during the design of those filters is to mitigate the oscillations that usually result from an attempt to continuously reduce the transition band (region between passband and stopband of filters) [5]. The finite-infinite dual and reversible relationship between time and frequency domain makes it hard to use this method for reducing the ripples in the finalized FIR filter designs. This actually could be a good area to explore for future research.

## Acknowledgements

My sincere thanks go to my three research advisors for their patience, their flexibility, and their support.

Special thanks to my friend Tirivanhu Chinyoka who taught me how to use Mathematica software, in addition to all the help he provided me with other aspects of my work.

## References

- [1] W Cai, D. Gottlieb & C.W. Shu, *Essentially Nonoscillatory Spectral Fourier Methods for Shock Wave Calculations*, Math. Comp., v. 52, **186**, 1989, pp. 389–410.
- [2] J Geer & N. Banerjee, *Exponentially Accurate Approximations to Piece-Wise Smooth Periodic Functions*, Math. Comp., v. 12, **3**, 1997, pp. 253–287.
- [3] M.A. Pinsky, *Introduction to Fourier Analysis and Wavelets*, Brooks/Cole, 2002.
- [4] C.M. Phillips & J.M Parr, *Signals, Systems and Transforms*, Prentice Hall, New Jersey, 1995.
- [5] L.B. Jackson, *Digital Filters and Signal Processing: with MATLAB Exercises*, Kluwer Academic Publishers, Norwell, 1995.